Supporting Information

Referential Tuning Strategy for High-Lying Triplet Energy Level Setting in OLED Emitter with Hot-exciton Characteristic

Qinqin Ke,[#a] Yuyue Song,[#a] Ganggang Li,[a] Baoxi Li,[a] Yiwen Chen,[a] Qing Wan,[c] Dongge Ma,*[a] Zhiming Wang*[a] and Ben Zhong Tang*[a,b]*

[a] *AIE Institute, State Key Laboratory of Luminescent Materials and Devices, Center for Aggregation-induced emission, Guangdong Provincial Key Laboratory of Luminescence from Molecular Aggregates (South China University of Technology), Guangzhou 510640, China.* wangzhiming@scut.edu.cn

[b] *Shenzhen Institute of Aggregate Science and Technology, School of Science and Engineering, The Chinese University of Hong Kong, Shenzhen, Guangdong 518172, China.* tangbenz@cuhk.edu.cn

[c] *School of Materials Science and Engineering, Nanchang Hangkong University, Nanchang 330063, China*

[#] *These authors contribute equally.*

1. General information

All the chemical agents and solvents were purchased from commercial sources and directly used as recceived. The final products were further purified by vacuum sublimation before the investigation of photoluminescence (PL) and electroluminescence (EL) properties. ^{1}H and ^{13}C NMR spectra were recorded on a Bruker AV 500 spectrometer in CD2Cl2 at room temperature. e. High resolution mass spectra (HRMS) were measured on a GCT premier CAB048 mass spectrometer operating in MALDI-TOF mode. A Shimadzu UV-2600 spectrophotometer was used for measurements of UV-vis absorption spectrum. PL spectra were tested on a Horiba Fluoromax-4 spectrofluorometer. Fluorescence quantum yields in solutions and solid states were measured using a Hamamatsu absolute PL quantum yield spectrometer C11347 Quantaurus_QY. Fluorescence lifetimes were determined on a Hamamatsu C11367-11 Quantaurus-Tau time-resolved spectrometer. Thermogravimetric analysis (TGA) analysis was performed on a TA TGA Q5000 under dry nitrogen at a heating rate of 10 ℃ min^{-1} from 30 ℃ to 800 ℃. Cyclic voltammogram (CV) was performed on a CHI 610E A14297 in a solution of tetra-n-butylammonium hexafluorophosphate (Bu_4NPF_6, 0.1 M) in dichloromethane (DCM) and dimethylformide (DMF) at a scan rate of 100 mV s^{-1}. Three-electrode system (Ag/Ag^+, platinum wire and glassy carbon electrode as reference, counter and work electrode respectively) was used in the CV method. HOMO = $-[E_{ox} + 4.8]$ eV, and LUMO = $-[E_{red} + 4.8]$ eV, where E_{ox} and E_{red} represent the onset oxidation and reduction potentials relative to Fe/Fe^+(4.8eV), respectively. The optimal ground structure and natural transition orbitals (NTOs) were calculated using the density function theory (DFT) and time-

dependent density function theory (TD-DFT) method with B3LYP at the basis set level of 6-31G (d,p). All the calculations were carried out using Gaussian 09 (version D.01) package.

2. Synthesis and characterization

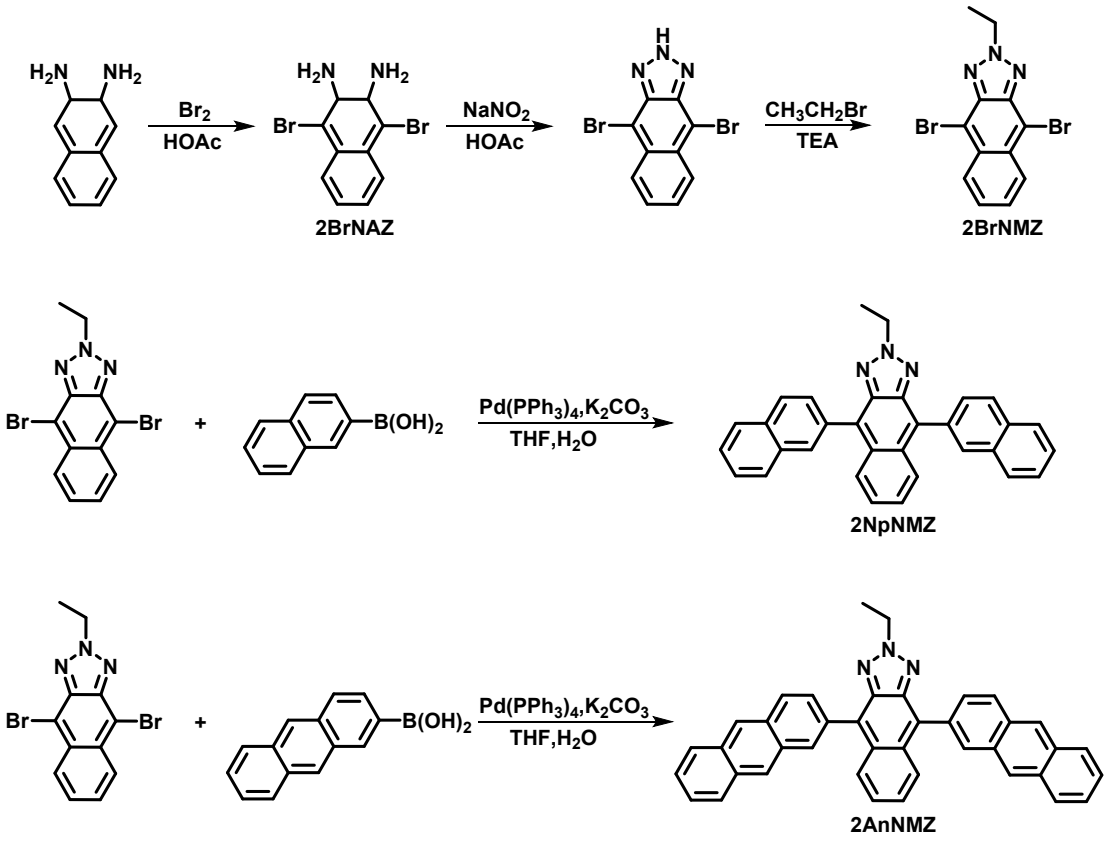

Scheme S1 synthesis routes of 2NpNMZ and 2AnNMZ emitters.

Synthesis of 2NpNMZ

Intermediate product 2BrNMZ was synthesized according to previous report.[1] A mixture of 2-naphthaeneboronic acid (3 mmol, 522 mg), 2BrNMZ (1 mmol, 353 mg), $Pd(PPh_3)_4$ (0.05 mmol, 57.75 mg) were added into two-neck bottle under nitrogen. Then Toluene (30 mL) and K_2CO_3 aqueous solution (2 M, 10 mL) were injected into the bottle, and the reaction mixture was refluxed at 110 ºC for 12 h. After cooled to room temperature, the mixture was extracted for three times with DCM. The pure product was received by silica-gel column chromatography using DCM/petroleum as the eluent to afford a yellow powder (406.5 mg): ^{1}H NMR (500 MHz, CD_2Cl_2) δ = 8.19 (d, 2H), 8.11-8.08 (m, 4H), 8.02-7.96 (m, 4H), 7.85-7.82 (m, 2H), 7.00 (t, 4H), 7.33-7.30 (m, 2H), 4.87-4.81 (q, 2H), 1.70-1.66 (t, 3H). ^{13}C NMR (126 MHz, CD_2Cl_2) δ = 144.28, 135.49, 134.69, 134.26, 131.63, 131.49, 130.56, 129.46, 129.11, 128.62,

127.72, 126.17, 69.07, 16.49. HRMS (C32H23N3): m/z 450.1967 [M+, calcd 450.1926].

Synthesis of 2AnNMZ

The synthetic routes were similar with 2NpNMZ, yellow powder was obtained (452.6 mg): ^{1}H NMR (500 MHz, CD_2Cl_2) δ = 8.61 (d, 4H), 8.39 (s, 2H), 8.28-8.08 (m, 8H), 7.87 (d, 2H), 7.55 (t, 4H), 7.37 (m, 2H), 4.89-4.85 (q, 2H), 1.72-1.69 (t, 3H). ^{13}C NMR (126 MHz, CD_2Cl_2) δ = 144.31, 134.99, 133.42, 132.86, 132.35, 131.82, 131.51, 130.39, 129.55, 129.35, 128.67, 128.01, 127.78, 127.51, 126.94, 126.25, 69.15, 16.53. HRMS (C40H27N3): m/z 550.22 [M+, calcd 549.22].

The structure of doped device:

ITO/HATCN (5 nm)/TAPC (50 nm)/TcTa (5 nm)/CBP: 10 wt% EML (20 nm)/TmPyPB (40 nm)/LiF (1 nm)/Al (120 nm), in which 4,4'-bis(N-carbazolyl)-1,1'-biphenyl (CBP) was chosen as a host matrix.

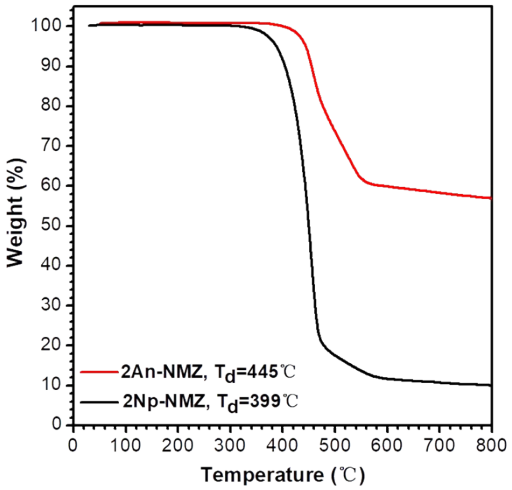

Fig. S1 The spectra of thermal decomposition temperature.

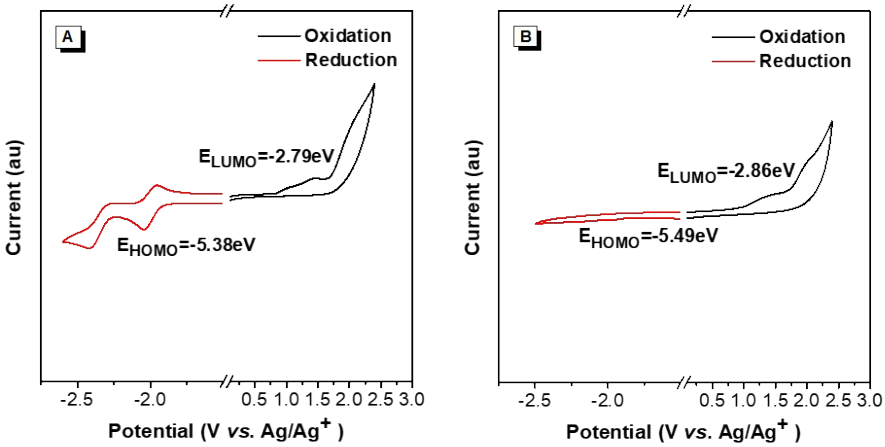

Fig. S2 Electrochemical property: (A) 2NpNMZ, (B) 2AnNMZ.

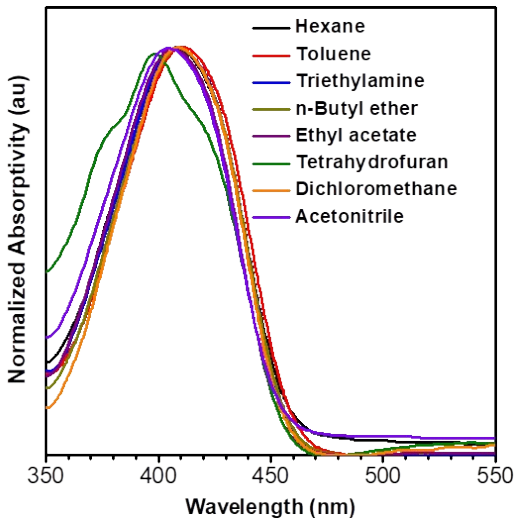

Fig. S3 UV-Vis absorption spectra of 2NpNMZ in various organic solvents. (Concentration: 10^{-5} M).

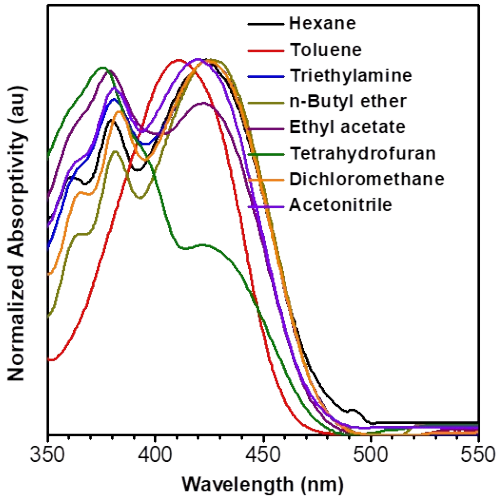

Fig. S4 UV-Vis absorption spectra of 2AnNMZ in various organic solvents. (Concentration: 10^{-5} M).

Table S1 Photophysical data of 2NpNMZ in different solvents.

Solvents	Δf	λ_{abs} [a] [nm]	λ_{em} [b] [nm]	Stokes shift [cm^{-1}]	Φ_F [c] [%]	Lifetime [d] [ns]
Hexane	0	409	493	4166	65.8	3.14
Triethylamine	0.048	409	496	4289	60.8	2.90
Butyl ether	0.096	409	496	4289	69.1	3.25
Ethyl Acetate	0.2	406	496	4469	69.6	3.23
Tetrahydrofuran	0.21	399	494	4820	50.2	3.30
Dichloromethane	0.217	409	493	4166	72.6	3.42
Dimethyl Formamide	0.276	410	497	4270	76.1	3.48
Acetonitrile	0.284	405	487	4157	67.4	3.36

[a] Absorption peak; [b] Emission peak; [c] Fluorescence quantum yield; [d] fluorescence lifetime.

Table S2 Photophysical data of 2AnNMZ in different solvents.

Solvents	Δf	λ_{abs} [a] [nm]	λ_{em} [b] [nm]	Stokes shift [cm^{-1}]	Φ_F [c] [%]	Lifetime [d] [ns]
Hexane	0	424	514	4130	72.3	2.74
Triethylamine	0.048	426	520	4243	65.8	2.71
Butyl ether	0.096	426	519	4206	69.4	2.77
Ethyl Acetate	0.2	422	521	4503	71.3	2.92
Tetrahydrofuran	0.21	422	520	4466	65.4	2.73
Dichloromethane	0.217	425	521	4336	75.4	2.91
Dimethyl Formamide	0.276	426	522	4317	72.2	3.10
Acetonitrile	0.284	419	518	4561	69.0	3.21

[a] Absorption peak; [b] Emission peak; [c] Fluorescence quantum yield; [d] fluorescence lifetime.

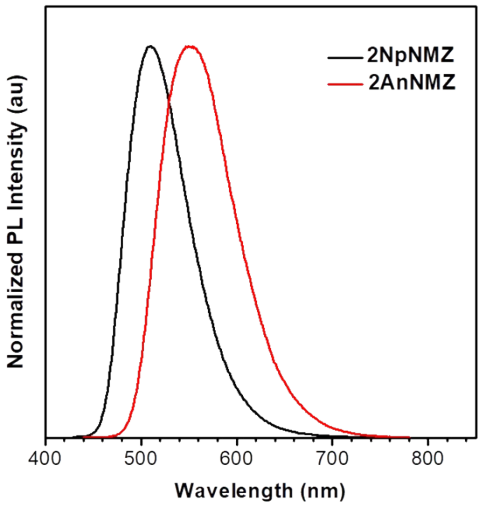

Fig. S5 PL spectra of 2NpNMZ and 2AnNMZ in the neat film. (Thickness: 20 nm).

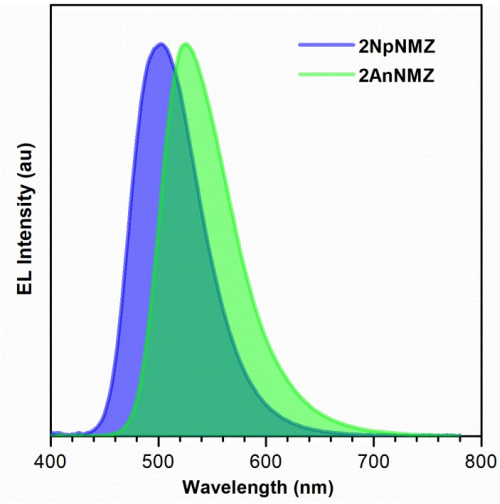

Fig. S6 EL spectra of doped devices.

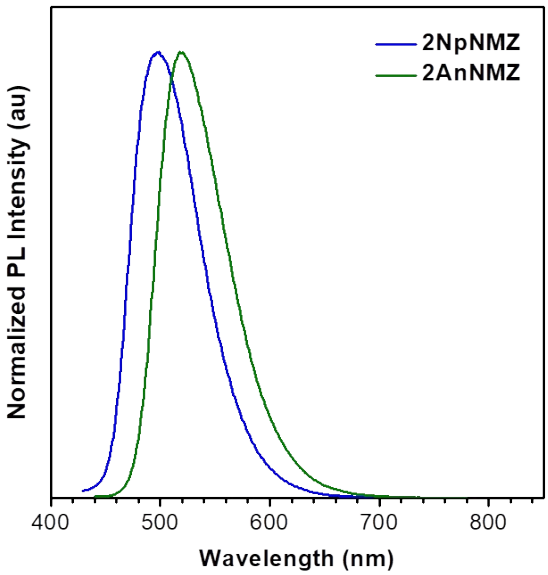

Fig. S7 PL spectra of doped devices.

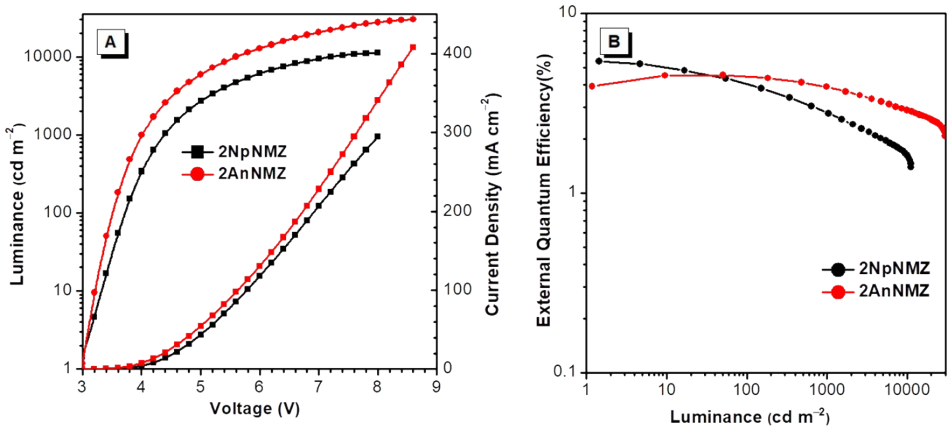

Fig. S8 (A) luminance–voltage–current density characteristics, (B) external quantum efficiency–brightness characteristics of the doped devices.

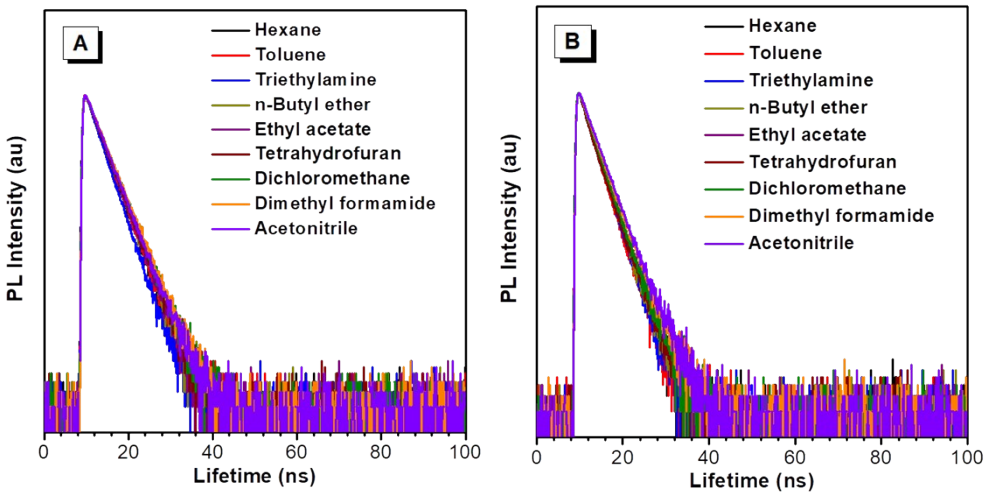

Fig. S9 Logarithmic decay curves in different solvents: (A) 2NpNMZ, (B) 2AnNMZ.

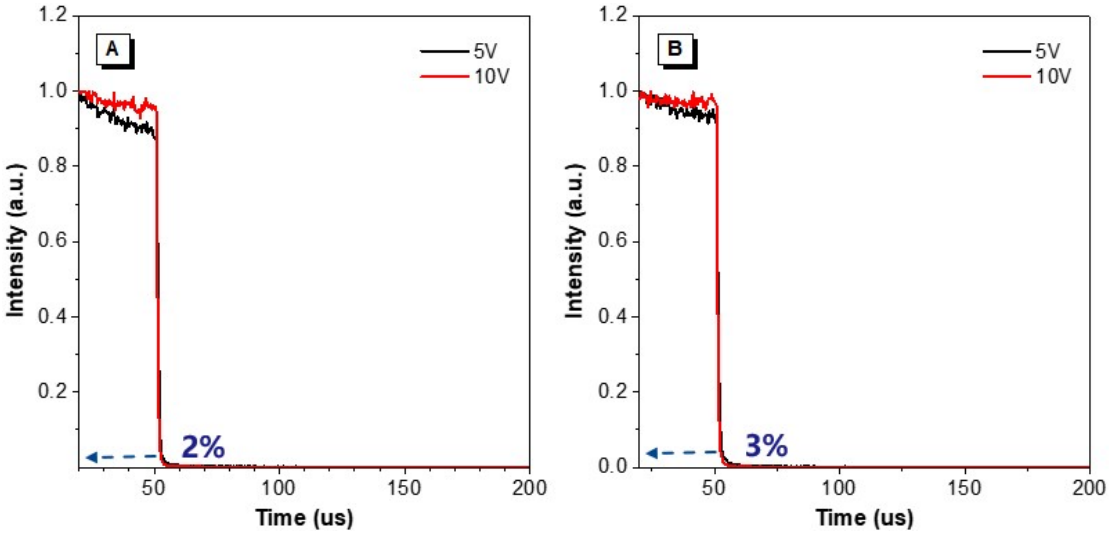

Fig. S10 Transient electroluminescence response of doped emitters (A) 2NpNMZ, (B)2AnNMZ.

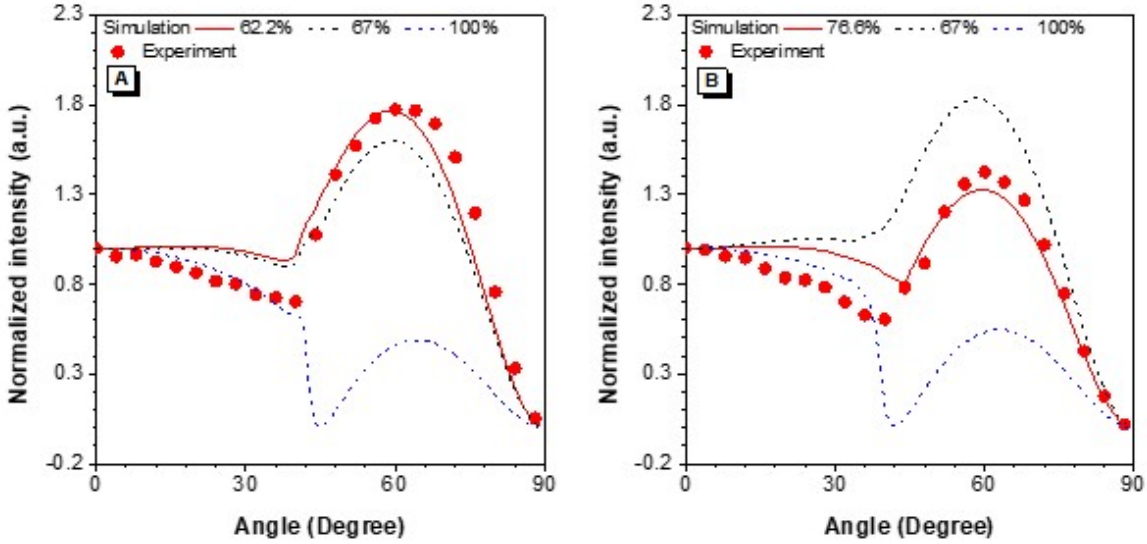

Fig. S11 The p-polarized PL intensity of the nondoped films of (A) 2NpNMZ and (B) 2AnNMZ.

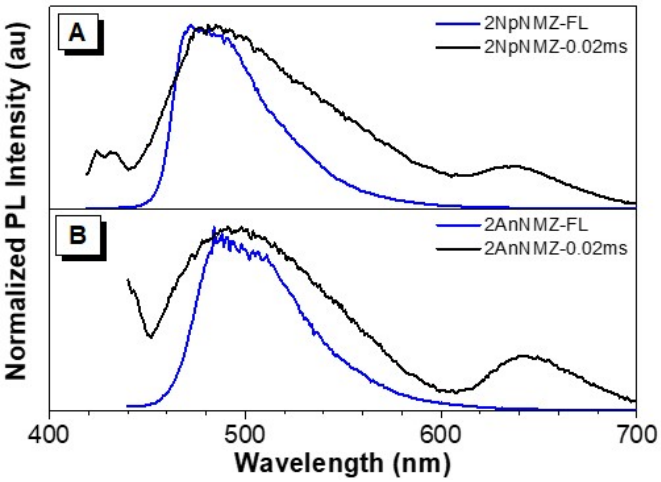

Fig. S12 Low-temperature fluorescent and phosphorescent spectra of (A) 2NpNMZ and (B) 2AnNMZ.

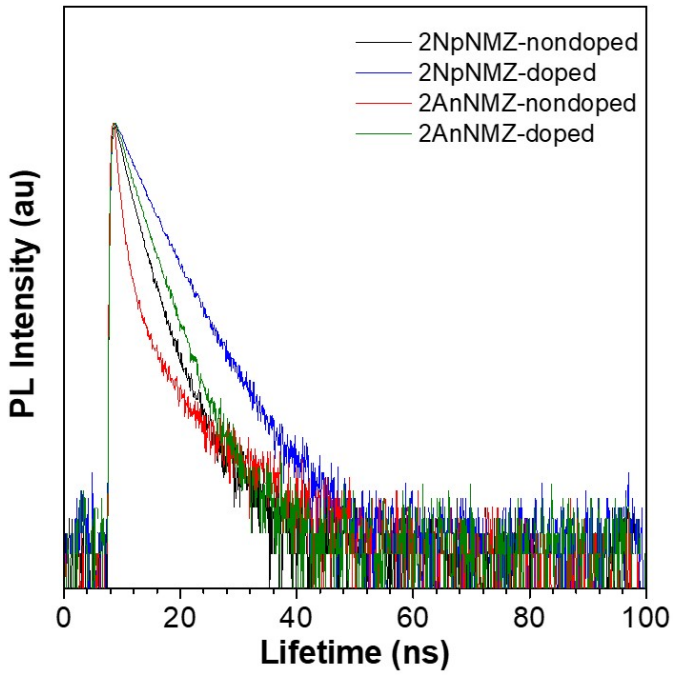

Fig S13 Normalized transient PL decay curves of doped/non-doped films

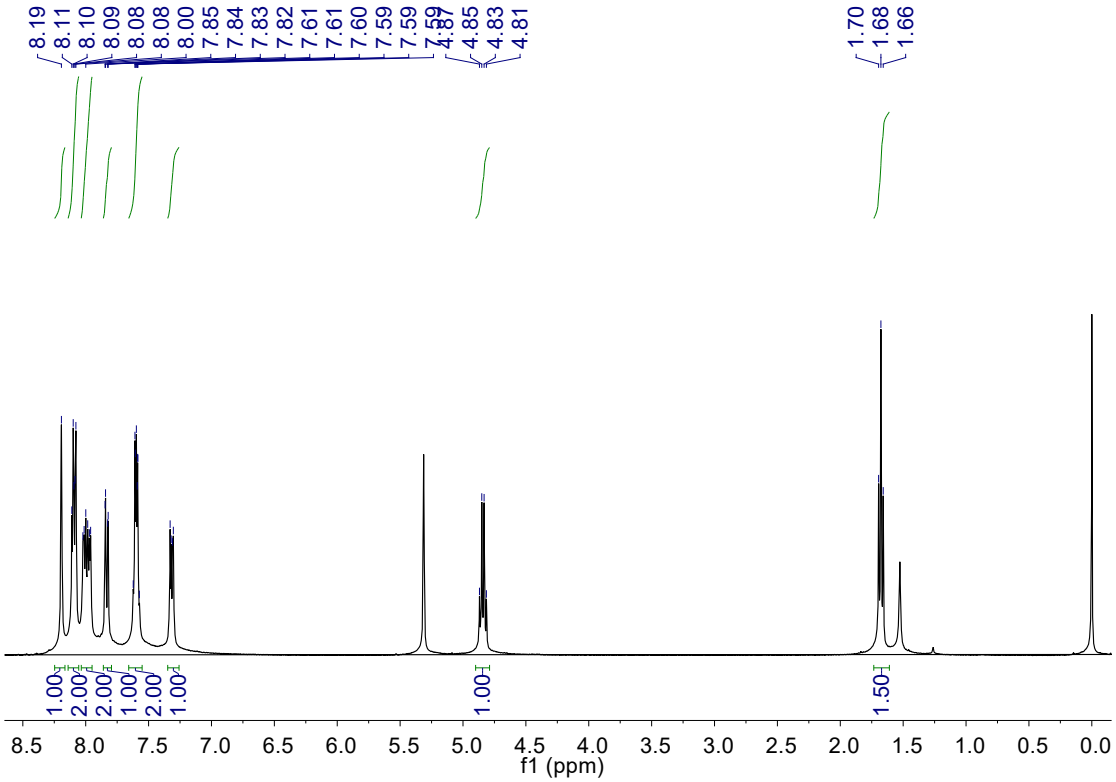

Fig. S14 ^{1}H NMR spectrum of 2NpNMZ in d-CD_2Cl_2.

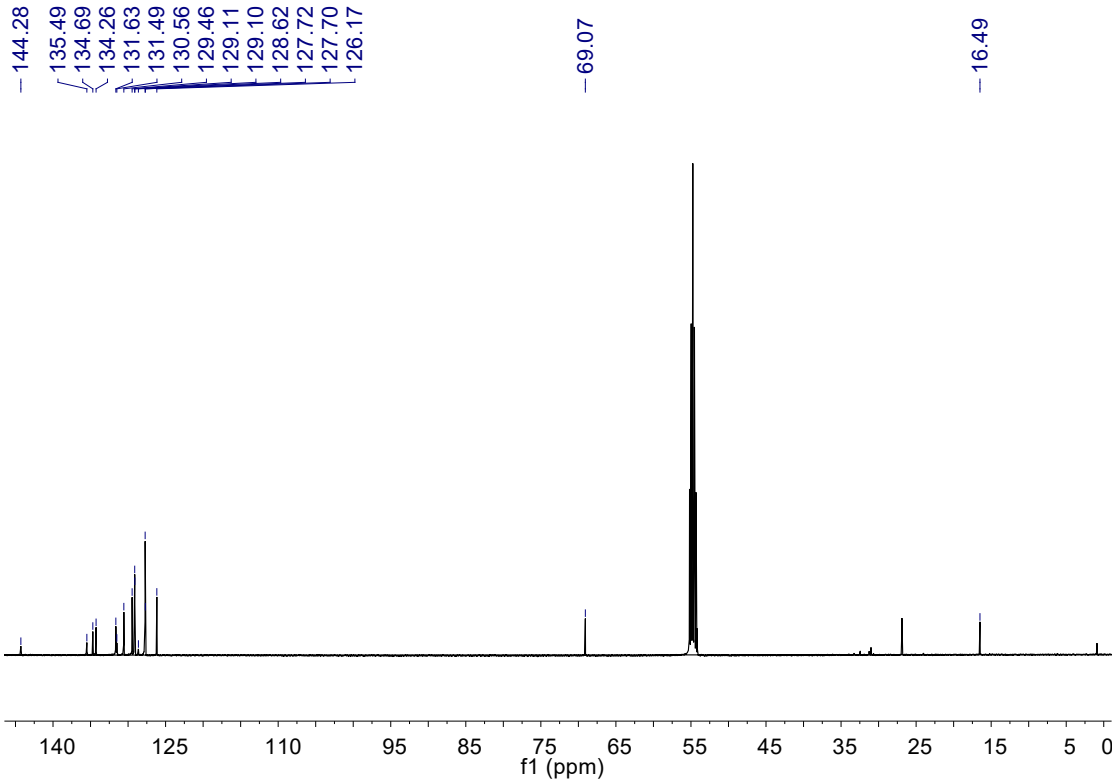

Fig. S15 ^{13}C NMR spectrum of 2NpNMZ in d-CD_2Cl_2.

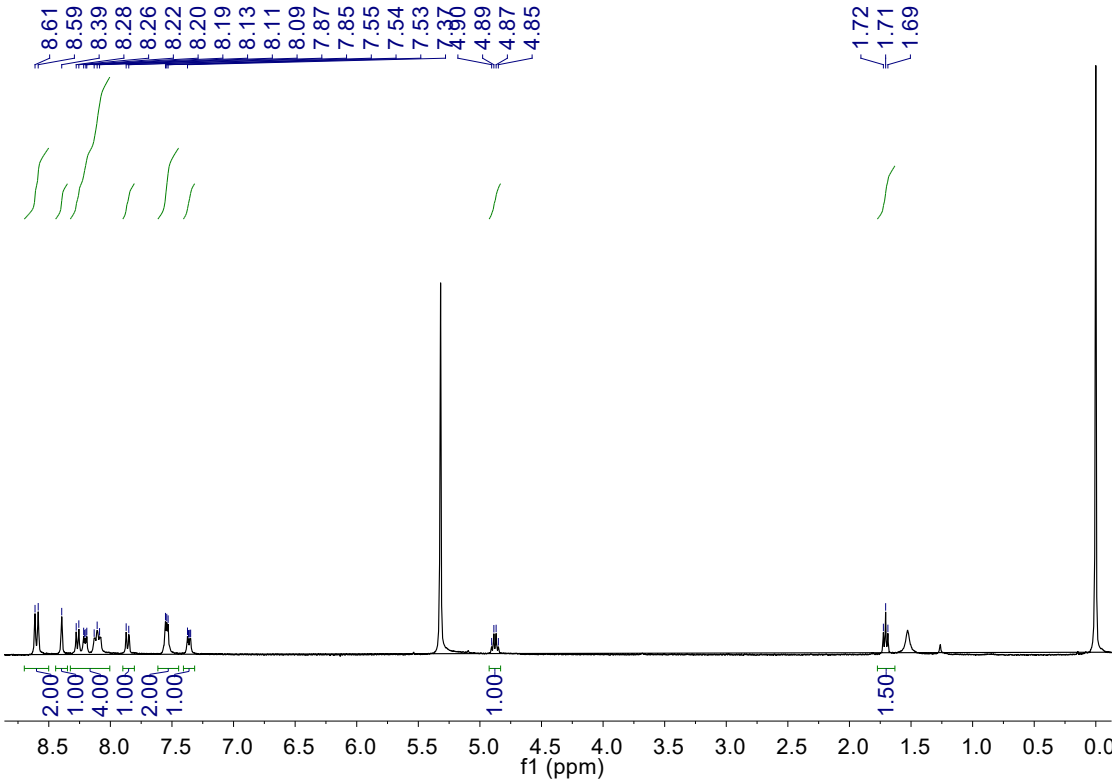

Fig. S16 ^{1}H NMR spectrum of 2AnNMZ in d-CD_2Cl_2.

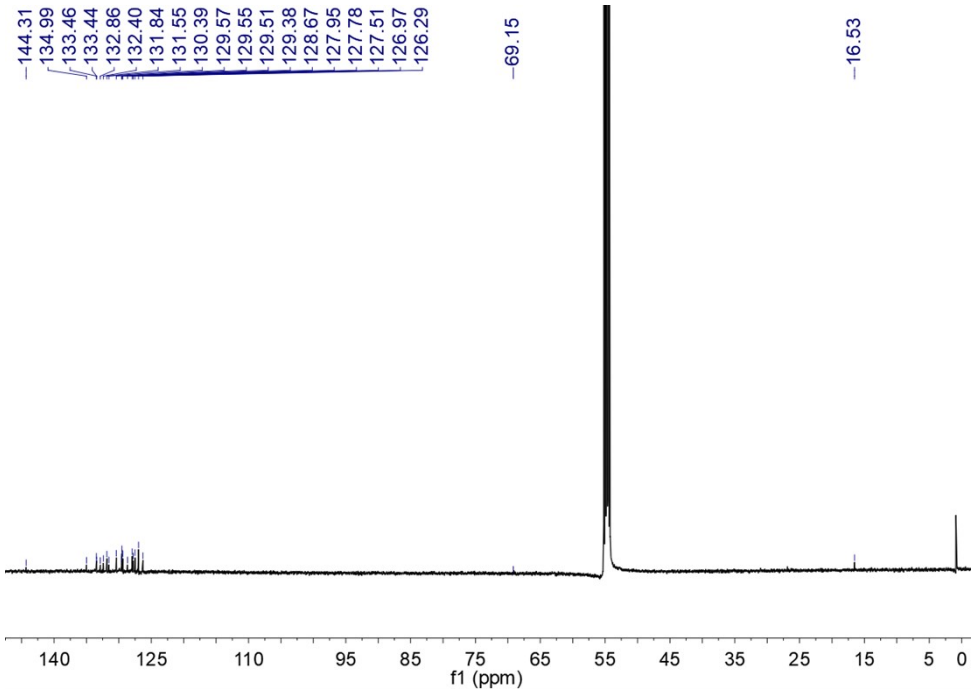

Fig. S17 ^{13}C NMR spectrum of 2AnNMZ in d-CD_2Cl_2.

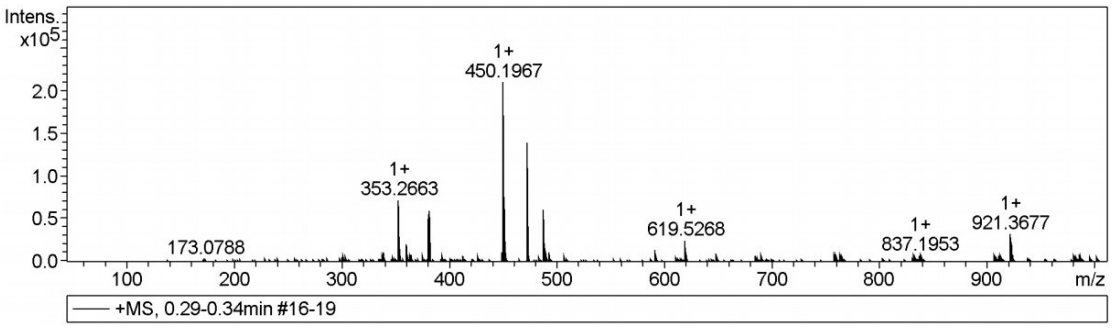

Fig. S18 HRMS of 2Np-NMZ.

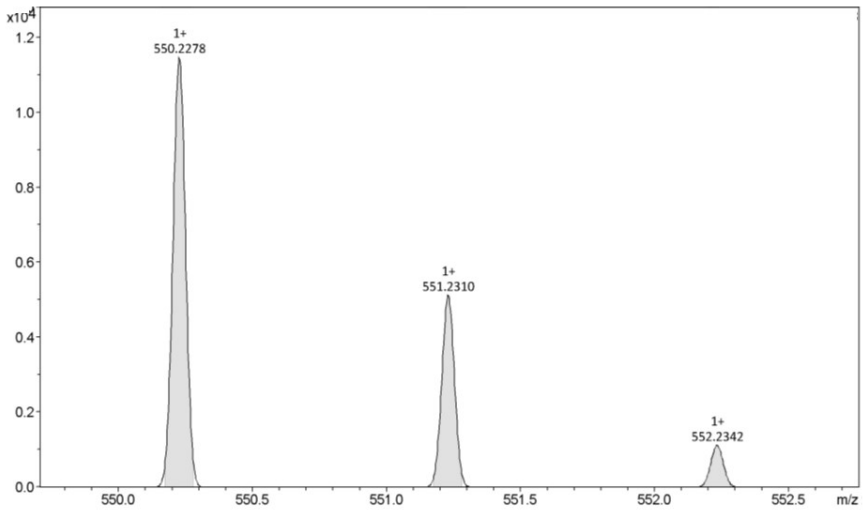

Fig. S19 HRMS spectrum of 2AnNMZ.